JOURNAL OF AGRICULTURAL AND FOOD CHEMISTRY

pubs.acs.org/JAFC

Article

Insights in the Recalcitrance of Theasinensin A to Human Gut Microbial Degradation

Zhibin Liu, Wouter J.C. de Bruijn, Mark G. Sanders, Sisi Wang, Marieke E. Bruins, and Jean-Paul Vincken*

Cite This: *J. Agric. Food Chem.* 2021, 69, 2477−2484

Read Online

ACCESS | Metrics & More | Article Recommendations | Supporting Information

ABSTRACT: Due to low bioavailability of dietary phenolic compounds in small intestine, their metabolism by gut microbiota is gaining increasing attention. The microbial metabolism of theasinensin A (TSA), a bioactive catechin dimer found in black tea, has not been studied yet. Here, TSA was extracted and purified for *in vitro* fermentation by human fecal microbiota, and epigallocatechin gallate (EGCG) and procyanidin B2 (PCB2) were used for comparison. Despite the similarity in their flavan-3-ol skeletons, metabolic fate of TSA was distinctively different. After degalloylation, its core biphenyl-2,2′,3,3′,4,4′-hexaol structure remained intact during fermentation. Conversely, EGCG and PCB2 were promptly degraded into a series of hydroxylated phenylcarboxylic acids. Computational analyses comparing TSA and PCB2 revealed that TSA's stronger interflavanic bond and more compact stereoconfiguration might underlie its lower fermentability. These insights in the recalcitrance of theasinensins to degradation by human gut microbiota are of key importance for a comprehensive understanding of its health benefits.

KEYWORDS: *theasinensins, gut microbiota, microbial degradation, UHPLC-Q-Orbitrap-MS, bond dissociation enthalpy*

INTRODUCTION

Black tea, as one of the most consumed beverages worldwide, has been reported to possess numerous health benefits.[1] The main bioactive compounds in black tea are generally considered to be the flavonoids, accounting for approximately 30% of the dry weight of black tea.[2] The unique constituents differentiating black tea from green tea are dimeric, oligomeric, and polymeric flavan-3-ols, such as theaflavins and theasinensins.[3] Due to the structural complexity of black tea phenolics, complete elucidation of their exact chemical structures and bioactivities is challenging. Therefore, selecting less complex compounds, which possess substructures representative for black tea phenolics is a commonly used approach to gain insights in their reactivity and bioactivity. During the oxidation process of catechins, two major oxidation pathways exist: (i) the condensation of a catechol-type B ring and a pyrogallol-type B ring to form a 1′,2′-dihydroxy-3,4-benzotropolone moiety, and (ii) the coupling of two pyrogallol-type B rings to form a biphenyl-2,2′,3,3′,4,4′-hexaol moiety.[3,4] The major oxidation products representing these two substructures include theaflavins and theasinensins. Hence, theaflavins and theasinensins could be used as the representatives to study black tea phenolics. So far, theaflavins have been studied to a greater extent than theasinensins, even though both are major contributors to the black tea phenolic content.

Theasinensins are a group of dimeric flavan-3-ols with an interflavanic C−C bond connecting two pyrogallol-type catechin B-rings. Five theasinensins have been identified from black tea and oolong tea, namely theasinensin A, B, C, D, and E (Figure 1). Among these five compounds, theasinensin A (TSA) is reported as the most abundant one.[5,6] Several studies have reported that theasinensins can

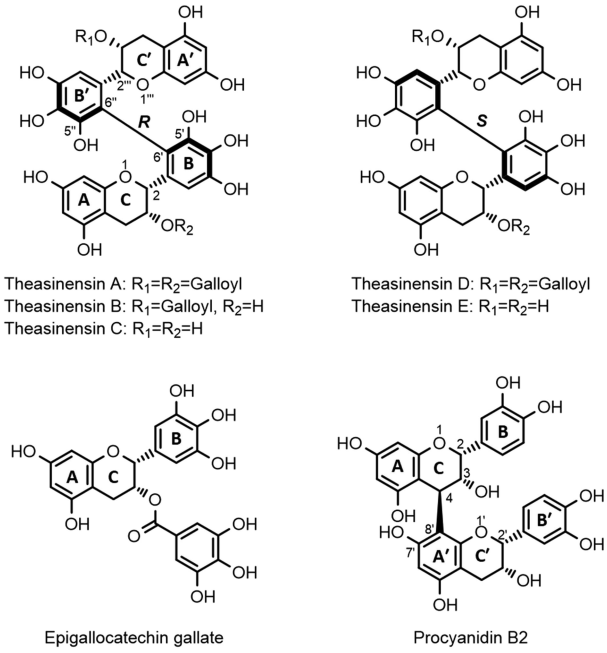

Figure 1. Chemical structure of theasinensins A−E, epigallocatechin gallate (EGCG), and procyanidin B2 (PCB2).

Received: February 3, 2021
Revised: February 10, 2021
Accepted: February 16, 2021
Published: February 23, 2021

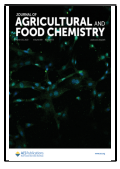

https://dx.doi.org/10.1021/acs.jafc.1c00727
J. Agric. Food Chem. 2021, 69, 2477−2484

exhibit health promoting effects.[7] For example, in an animal study with type 2 diabetic male KK-A^y mice, Miyata *et al.* observed that the addition of 0.1% (w/w) TSA (purity 59%) to the mice's diet for 6 weeks resulted in a >30% reduction of serum glucose levels in comparison with a control diet.[8] However, it has also been reported that tea phenolics are poorly absorbed in the small intestine and pass into the colon where they are subject to metabolism by gut microbiota.[9] Thus, microbial metabolism may play a critical role in the digestion and bioactivity of theasinensins. However, to the best of the authors' knowledge, there have been no reports so far on the metabolic fate of theasinensins in the colon.

On the other hand, studies on the microbial metabolism of monomeric flavan-3-ols, such as epigallocatechin gallate (EGCG, Figure 1), are abundant. In general, the bioconversion of catechins can be summarized as follows: galloyl ester hydrolysis (if applicable) is succeeded by consecutive C-ring opening, A-ring fission, dehydroxylation, and aliphatic chain shortening. This eventually results in degradation of catechins to a series of smaller metabolites, such as phenylvalerolactones, phenylvaleric acids, phenylpropionic acids, phenylacetic acids, and benzoic acids.[4,10−12] It has also been reported that B-type procyanidin dimers, such as procyanidin B2 (PCB2, Figure 1), which consist of two catechin subunits linked via an interflavanic C−C bond between one of the A and one of the C rings, could be converted into similar metabolites.[13] Considering the structural similarities between theasinensins and B-type procyanidins, it is expected that theasinensins will be subject to similar microbial conversions. However, it is unclear to which extent theasinensins can be degraded by human gut microbiota.

The aim of this study was to investigate the metabolic fate of theasinensins. To this end, purified TSA was incubated with human fecal microbiota under anaerobic conditions, and its metabolites were monitored by UHPLC-Q-Orbitrap-MS. Additionally, the same treatment was performed with EGCG and PCB2 for comparison. Furthermore, a computational study was performed with theasinensins and PCB2 to compare the stereo-configurations and bond strength of several potential microbial cleavage sites.

MATERIALS AND METHODS

Chemicals. Standards of epicatechin (EC), epigallocatechin (EGC), epicatechin gallate (ECG), epigallocatechin gallate (EGCG), procyanidin B2 (PCB2), gallic acid, pyrogallol, benzoic acid, 4-hydroxybenzoic acid, 3-(4′-hydroxyphenyl)propionic acid, 3-(3′-hydroxyphenyl)propionic acid, 3-(3′,4′-dihydroxyphenyl)-propionic acid, 4-hydroxyphenylacetic acid, 4-phenylbutyric acid, 5-(4′-hydroxyphenyl)valeric acid, and 5-phenylvaleric acid were purchased from Sigma Aldrich (St. Louis, MO, USA). Ultrahigh-performance liquid chromatography/mass spectrometry grade acetonitrile (ACN), ACN with 0.1% (v/v) formic acid, and water with 0.1% (v/v) formic acid were purchased from Biosolve (Valkenswaard, The Netherlands). Water delivered by Milli-Q water purification system (Millipore, Billerica, MA, USA) was used for other purposes than LC−MS.

Extraction and Purification of TSA. It was reported that TSA occurred abundantly in black tea and oolong tea.[7,14] To select the most suitable raw material for TSA purification, the TSA content in 15 black tea samples and 6 oolong tea samples was compared. The Lapsang Souchong black tea sample contained the highest TSA content (7.07 mg TSA/g DW), thus, this tea was selected for purification of TSA. The results of TSA quantification in all tea samples are shown in Table S1, Supporting Information. In the further extraction of TSA, dry leaves (15 g) were cut into small pieces (approximately 5 mm in length) and extracted twice with 500 mL of acetone/water (50:50, v/v) by ultra-sonication for 30 min at room temperature. After filtration over a paper filter (Whatman, Maidstone, UK), the black tea extracts were combined and the organic solvent was evaporated under reduced pressure. Subsequently, the aqueous solution was decaffeinated by liquid−liquid partitioning with an equal volume of chloroform for 30 min. The aqueous phase was collected and centrifuged (20 min, 3000 × g). The supernatant was collected and lyophilized to yield the cleaned extract. The cleaned extract was then pre-purified using a Reveleris flash chromatography system (Grace, Columbia, USA). Next, a Waters preparative RP-HPLC system (Waters, Milford, MA, USA) was used for the further purification of the pools obtained from flash chromatography. The details of the methods used for purification of TSA by flash chromatography and preparative RP-HPLC are described in the Supporting Information. The purity of the obtained TSA was analyzed based on peak purity analysis using a photo diode array (PDA) detector at 280 nm in UHPLC-PDA-ESI-IT-MS. The structure of the obtained TSA was confirmed by UHPLC-Q-Orbitrap-MS and nuclear magnetic resonance (NMR) spectrometry. The NMR method is described in the Supporting Information.

Tannase Treatment of TSA to Obtain Theasinensins B and C. To obtain mass spectrometric information of theasinensin B (TSB, single degalloylation product of TSA) and theasinensin C (TSC, double degalloylation product of TSA), TSA was degallolylated with tannase. A 500 μL aqueous TSA solution (1.0 mmol/L) was incubated with 500 μL tannase (0.15 U/mL, from *Aspergillus ficuum*, Sigma Aldrich) for 30 min at room temperature. The resulting mixture, containing TSB and TSC, was analyzed by UHPLC-Q-Orbitrap-MS. In addition, to obtain solely TSC, an excess of tannase (900 μL, 0.15 U/mL) was added to an aqueous TSA solution (100 μL, 1.0 mmol/L) for 24 h at room temperature. The resulting solution was used as a TSC standard for identification and quantification.

***In Vitro* Fermentation with Human Gut Microbiota.** Fecal materials obtained from four healthy volunteers (3 males and 1 female, 24 to 38 years old, no tea consumption in the week prior to donation antibiotic treatment in 3 months prior to the donation) were pooled and used for the fecal fermentation of TSA, EGCG, and PCB2. The fermentations were performed following the same procedure as described previously.[12] The final concentrations of TSA, EGCG, and PCB2 were 50, 100, and 50 μmol/L, respectively. For UHPLC-Q-Orbitrap-MS analysis, a fermentation sample of 100 μL was taken after 0, 2, 6, 12, 24, 36, and 48 h of fermentation and immediately diluted in 300 μL of ACN to stop the fermentation. All fermentations were performed in triplicate.

UHPLC-Q-Orbitrap-MS Analysis of the Degradation Pathway. A Vanquish UHPLC system (Thermo Fisher Scientific, Bremen, Germany) equipped with a binary pump, split loop autosampler, column compartment, and diode array detector was used for chromatographic separations. The UHPLC system was coupled in line to a Thermo Q-Exactive Focus hybrid quadrupole-Orbitrap mass spectrometer (Thermo Fisher Scientific, Bremen, Germany) equipped with a heated ESI source. The analytical methods used for chromatographic separation and mass spectrometric analysis of the samples are described elsewhere.[12]

External standards of TSA, EGCG, PCB2, ECG, EGC, EC, gallic acid, pyrogallol, benzoic acid, 4-hydroxybenzoic acid, 3-(3′,4′-dihydroxyphenyl)propionic acid, 4-hydroxyphenylacetic acid, 4-phenylbutyric acid, 5-(4′-hydroxyphenyl)valeric acid, 3-(4′-hydroxyphenyl)propionic acid, and 5-phenylvaleric acid were used for quantification and qualification of the detected metabolites. The concentrations of these compounds and compounds with similar structures were determined based on the respective external calibration curves (6.25 to 100 μmol/L, $R^2 > 0.99$).

Computational Analysis. To compare the geometrical conformations and the bond strength of several potential microbial cleavage sites (interflavanic bonds and C-ring O1−C2 bonds) between theasinensins (TSA and TSC) and PCB2, density functional theory (DFT) calculations were performed. Geometrical optimization

https://dx.doi.org/10.1021/acs.jafc.1c00727
J. Agric. Food Chem. 2021, 69, 2477−2484

Table 1. Tentative Identifications and Dynamic Changes of Metabolites of TSA, EGCG and PCB2 during Fermentation with HFS

id	RT (min)	Tentative identification [a]	Formula	$[M-H]^-$ (m/z)	Δ m/z (ppm)	Source	Concentration at different fermentation times (μmol/L) [c]						
							0 h	2 h	6 h	12 h	24 h	36 h	48 h
M01	5.35	Theasinensin B	$C_{37}H_{30}O_{18}$	761.13617	-0.31	TSA	n.d.	n.d.	1.15	10.68	16.16	6.94	n.d.
						EGCG	n.d.	n.d.	n.d.	n.d.	n.d.	n.d.	n.d.
						PCB2	n.d.	n.d.	n.d.	n.d.	n.d.	n.d.	n.d.
M02	2.30	Theasinensin C	$C_{30}H_{26}O_{14}$	609.12500	-0.03	TSA	n.d.	n.d.	n.d.	3.12	18.29	30.62	41.61
						EGCG	n.d.	n.d.	n.d.	n.d.	n.d.	n.d.	n.d.
						PCB2	n.d.	n.d.	n.d.	n.d.	n.d.	n.d.	n.d.
M03	5.16	Theasinensin E	$C_{30}H_{26}O_{14}$	609.12506	-0.13	TSA	n.d.	n.d.	n.d.	n.d.	n.d.	n.d.	4.95
						EGCG	n.d.	n.d.	n.d.	n.d.	n.d.	n.d.	n.d.
						PCB2	n.d.	n.d.	n.d.	n.d.	n.d.	n.d.	n.d.
M04	5.75	Epigallocatechin [b]	$C_{15}H_{14}O_7$	305.06680	-0.41	TSA	n.d.	n.d.	n.d.	n.d.	n.d.	n.d.	n.d.
						EGCG	3.09	5.44	0.13	n.d.	n.d.	n.d.	n.d.
						PCB2	n.d.	n.d.	n.d.	n.d.	n.d.	n.d.	n.d.
M05	6.71	Epicatechin [b]	$C_{15}H_{14}O_6$	289.07181	-0.17	TSA	0.03	n.d.	n.d.	n.d.	n.d.	n.d.	n.d.
						EGCG	0.11	n.d.	n.d.	n.d.	n.d.	n.d.	n.d.
						PCB2	0.04	3.05	n.d.	n.d.	n.d.	n.d.	n.d.
M06	6.80	1-(3′,4′,5′-Trihydroxyphenyl)-3-(2″,4″,6″-trihydroxyphenyl)-propan-2-yl gallate	$C_{22}H_{20}O_{11}$	459.09369	-0.88	TSA	n.d.	n.d.	n.d.	n.d.	n.d.	n.d.	n.d.
						EGCG	n.d.	0.09	0.55	0.07	n.d.	n.d.	n.d.
						PCB2	n.d.	n.d.	n.d.	n.d.	n.d.	n.d.	n.d.
M07	5.95	1-(3′,4′,5′-Trihydroxyphenyl)-3-(2″,4″,6″-trihydroxyphenyl)-propan-2-ol	$C_{15}H_{16}O_7$	307.08252	-0.64	TSA	n.d.	0.01	n.d.	n.d.	n.d.	n.d.	n.d.
						EGCG	n.d.	11.39	0.48	n.d.	n.d.	n.d.	n.d.
						PCB2	n.d.	n.d.	n.d.	n.d.	n.d.	n.d.	n.d.
M08	6.87	1-(3′,4′-Dihydroxyphenyl)-3-(2″,4″,6″-trihydroxyphenyl)-propan-2-ol	$C_{15}H_{16}O_6$	291.08762	-0.71	TSA	n.d.	n.d.	n.d.	n.d.	n.d.	n.d.	n.d.
						EGCG	n.d.	0.27	n.d.	n.d.	n.d.	n.d.	n.d.
						PCB2	n.d.	11.90	n.d.	n.d.	n.d.	n.d.	n.d.
M09	7.83	2-(3-(3,4-Dihydroxyphenyl)-2-hydroxy-1-(2,4,6-trihydroxyphenyl)propyl)-4-(3-(3,4-dihydroxyphenyl)-2-hydroxypropyl)benzene-1,3,5-triol	$C_{30}H_{30}O_{12}$	581.16687	0.72	TSA	n.d.	0.03	0.11	n.d.	n.d.	n.d.	n.d.
						EGCG	n.d.	n.d.	n.d.	n.d.	n.d.	n.d.	n.d.
						PCB2	n.d.	0.66	2.58	1.43	0.10	n.d.	n.d.
M10	7.68	2-(3,4-Dihydroxyphenyl)-8-(3-(3,4-dihydroxyphenyl)-2-hydroxy-1-(2,4,6-trihydroxyphenyl)propyl)chromane-3,5,7-triol	$C_{30}H_{28}O_{12}$	579.15143	1.09	TSA	n.d.	0.02	n.d.	n.d.	n.d.	n.d.	n.d.
						EGCG	n.d.	n.d.	n.d.	n.d.	n.d.	n.d.	n.d.
						PCB2	n.d.	3.26	0.92	0.44	n.d.	n.d.	n.d.
M11	8.78	2-(3-(3,4-Dihydroxyphenyl)-2-hydroxy-1-(2,4,6-trihydroxyphenyl)propyl)-4-(2-hydroxy-3-(3-hydroxyphenyl)propyl)benzene-1,3,5-triol	$C_{30}H_{28}O_{11}$	563.15564	-0.44	TSA	n.d.	n.d.	n.d.	n.d.	n.d.	n.d.	n.d.
						EGCG	n.d.	n.d.	n.d.	n.d.	n.d.	n.d.	n.d.
						PCB2	n.d.	n.d.	0.07	0.54	1.05	1.35	2.20
M12	5.99	5-(3′,4′,5′-Trihydroxyphenyl)-γ-valerolactone	$C_{11}H_{12}O_5$	223.06055	2.89	TSA	n.d.	n.d.	n.d.	n.d.	n.d.	n.d.	0.01
						EGCG	n.d.	0.01	0.69	0.27	0.67	1.16	1.77
						PCB2	n.d.	n.d.	0.49	n.d.	n.d.	n.d.	n.d.
M13	6.69	5-(3′,4′-Dihydroxyphenyl)-γ-valerolactone	$C_{11}H_{12}O_4$	207.06607	1.03	TSA	n.d.	n.d.	n.d.	n.d.	n.d.	n.d.	n.d.
						EGCG	n.d.	n.d.	0.14	0.94	1.52	1.77	1.67
						PCB2	n.d.	n.d.	n.d.	n.d.	n.d.	n.d.	n.d.
M14	7.80	5-(4′-Hydroxyphenyl)-γ-valerolactone	$C_{11}H_{12}O_3$	191.07103	1.75	TSA	n.d.	n.d.	n.d.	n.d.	n.d.	n.d.	n.d.
						EGCG	n.d.	n.d.	n.d.	n.d.	0.18	0.43	0.81
						PCB2	n.d.	n.d.	n.d.	n.d.	n.d.	n.d.	n.d.
M15	5.02	4-Hydroxy-5-(3′,4′,5′-trihydroxyphenyl)-valeric acid	$C_{11}H_{14}O_6$	241.07146	1.25	TSA	n.d.	n.d.	n.d.	n.d.	n.d.	n.d.	n.d.
						EGCG	n.d.	n.d.	3.97	1.34	0.25	0.05	n.d.
						PCB2	n.d.	n.d.	n.d.	n.d.	n.d.	n.d.	n.d.
M16	5.96	4-Hydroxy-5-(3′,4′-dihydroxyphenyl)-valeric acid	$C_{11}H_{14}O_5$	225.07631	2.39	TSA	n.d.	n.d.	n.d.	0.01	0.01	0.02	0.04
						EGCG	n.d.	n.d.	0.44	0.59	0.19	0.01	n.d.
						PCB2	n.d.	0.11	8.06	0.33	0.07	0.05	0.08
M17	5.65	5-(3′,4′,5′-Trihydroxyphenyl)-valeric acid	$C_{11}H_{14}O_5$	225.07632	2.33	TSA	n.d.	0.01	n.d.	n.d.	n.d.	n.d.	n.d.
						EGCG	0.01	0.01	1.07	5.98	11.13	6.56	1.76
						PCB2	0.01	n.d.	n.d.	0.01	n.d.	0.01	n.d.
M18	7.80	5-(3′,5′-Dihydroxyphenyl)-valeric acid	$C_{11}H_{14}O_4$	209.08165	1.36	TSA	0.02	0.02	n.d.	n.d.	n.d.	n.d.	0.02
						EGCG	0.02	0.01	n.d.	1.66	33.66	67.02	124.87 [d]
						PCB2	0.02	0.01	n.d.	0.01	0.01	0.02	0.03
M19	8.52	5-(3′,4′-dihydroxyphenyl)-valeric acid	$C_{11}H_{14}O_4$	209.08164	1.40	TSA	0.12	0.14	0.01	0.01	0.01	0.05	0.31
						EGCG	0.11	0.15	0.01	0.23	2.37	3.43	6.13
						PCB2	0.11	0.13	2.64	23.16	24.16	25.69	32.94
M20	9.92	5-(4′-Hydroxyphenyl)-valeric acid [b]	$C_{11}H_{14}O_3$	193.08691	0.56	TSA	0.28	0.33	0.17	0.20	0.25	0.31	0.42
						EGCG	0.24	0.35	0.15	0.20	0.35	0.92	5.14
						PCB2	0.24	0.35	0.17	0.64	5.85	9.32	20.33
M21	5.81	3-(3′,5′-Dihydroxyphenyl)-propionic acid	$C_9H_{10}O_4$	181.05032	1.73	TSA	n.d.	n.d.	n.d.	n.d.	n.d.	n.d.	0.01
						EGCG	n.d.	n.d.	n.d.	0.01	0.02	0.05	0.10
						PCB2	n.d.	n.d.	n.d.	n.d.	n.d.	n.d.	n.d.
M22	6.31	3-(3′,4′-dihydroxyphenyl)-propionic acid [b]	$C_9H_{10}O_4$	181.05040	1.29	TSA	n.d.	n.d.	n.d.	n.d.	n.d.	n.d.	n.d.
						EGCG	n.d.	n.d.	n.d.	n.d.	n.d.	n.d.	0.01
						PCB2	n.d.	n.d.	n.d.	n.d.	n.d.	n.d.	n.d.
M23	7.80	3-(3′-Hydroxyphenyl)-propionic acid [b]	$C_9H_{10}O_3$	165.05543	1.72	TSA	n.d.	n.d.	n.d.	n.d.	0.06	0.06	0.09
						EGCG	n.d.	n.d.	n.d.	n.d.	0.04	0.04	0.07
						PCB2	n.d.	n.d.	n.d.	0.01	0.13	0.17	0.28
M24	2.38	Gallic acid	$C_7H_6O_5$	169.01403	1.28	TSA	0.83	1.51	8.38	7.51	8.55	13.11	4.19
						EGCG	0.55	5.47	14.78	10.32	7.21	7.83	0.55
						PCB2	n.d.	n.d.	0.02	0.02	0.01	n.d.	n.d.
M25	5.82	4-Hydroxybenzoic acid	$C_7H_6O_3$	137.02398	3.19	TSA	0.03	0.03	0.02	0.11	0.17	0.21	0.29
						EGCG	0.05	0.05	0.03	0.04	0.07	0.10	0.14
						PCB2	0.05	0.06	0.03	0.05	0.08	0.10	0.16
M26	2.80	Pyrogallol	$C_6H_6O_3$	125.02412	2.35	TSA	0.03	0.06	0.56	1.85	10.65	25.32	27.92
						EGCG	0.03	0.16	7.53	12.57	10.15	8.49	7.63
						PCB2	n.d.	n.d.	n.d.	n.d.	n.d.	n.d.	n.d.

[a]Supporting mass spectrometric data can be found in Table S2, Supporting Information. [b]These identifications were confirmed with authentic standards. [c]Mean value of compound concentrations (n = 3) and n.d., not detected. The colors range from light blue to dark blue indicating the range from low to high relative concentration for each metabolite detected in all samples. [d]The quantification of this compound was calculated based on 5-(4′-hydroxyphenyl)valeric acid, which may have different response factors, and thus resulted in overestimation in the concentration.

https://dx.doi.org/10.1021/acs.jafc.1c00727
J. Agric. Food Chem. 2021, 69, 2477−2484

and frequency analysis of TSA, TSC, PCB2, and related radicals were calculated using Gaussian 09 software package at the DFT//B3LYP/6-311G(d,p) theoretical level, combined with a conductor-like polarizable continuum model (CPCM) for water at 298.15 K. The B3LYP model with the 6-311G(d,p) basis set was chosen because it was reported to be suitable for phenolic compounds.[15] Subsequently, the bond dissociation enthalpy (BDE) of the interflavanic C−C bond in each phenolic compound was computed. BDE is defined as the enthalpy change between the product radicals formed by the homolytic fission of a chemical bond and the starting reactant.[16] It is a widely used thermodynamic parameter for the estimation of the strength of chemical bonds. Theoretically, the homolytic fission of interflavanic bonds of TSA, TSC, or PCB2 will form two monomeric flavan-3-ol radicals. BDE of the interflavanic bond was described by the following equations:

$$\mathrm{BDE}_{\mathrm{TSA}} = H(\mathrm{EGCG}\cdot) + H(\mathrm{EGCG}\cdot) - H(\mathrm{TSA}) \quad (1)$$

$$\mathrm{BDE}_{\mathrm{TSC}} = H(\mathrm{EGC}\cdot) + H(\mathrm{EGC}\cdot) - H(\mathrm{TSC}) \quad (2)$$

$$\mathrm{BDE}_{\mathrm{PCB2}} = H(\mathrm{EC}\cdot) + H(\mathrm{EC}\cdot) - H(\mathrm{PCB2}) \quad (3)$$

All the molecular enthalpies (H) were calculated by using Gaussian 09.

RESULTS AND DISCUSSION

Purification and Identification of TSA. Liquid−liquid extraction of the crude black tea extract with chloroform efficiently removed 90% of the caffeine, without affecting the phenolic profile (data not shown). After decaffeination, the phenolic profile of the black tea extracts (Figure S1-A1,B1, Supporting Information) was comparable to that reported in other studies. After pre-purification by flash chromatography, a pool enriched in TSA was obtained, which still contained several other phenolics, such as *p*-coumaroylquinic acid, EGCG, kaempferol-deoxyhexosyldeoxyhexoside, and quercetin-hexoside (Figure S1-A2,B2, Supporting Information). After purification by preparative RP-HPLC separation, 20.4 mg of TSA was obtained from 15 g of black tea (Figure S1-A3,B3, Supporting Information). The purity of TSA was approximately 99% based on peak purity analysis using a PDA detector in UHPLC-PDA-ESI-IT-MS. The structure of TSA was confirmed based on high-resolution Q-Orbitrap-MS and NMR spectroscopy. In Q-Orbitrap-MS analysis, this compound was detected as its $[M - H]^-$ and $[M + H]^+$ ions with respective m/z values of 913.14731 and 915.16095, which were in agreement with its theoretical deprotonated and protonated monoisotopic accurate masses ($\Delta m/z$ of 0.45 and −0.49 ppm, respectively). Its HCD spectrum and corresponding fragmentation pathways in both negative and positive ionization modes are shown in Figure S2, Supporting Information. Its structure was further confirmed with ^{1}H, ^{13}C, heteronuclear single quantum coherence (HSQC) and heteronuclear multiple bond correlation (HMBC) NMR spectra (Figure S3, Supporting Information). The spectroscopic data of ^{1}H and ^{13}C NMR was in line with the published data.[17−19]

Degradation of TSA by Human Gut Microbiota. Purified TSA was then used for the fermentation by human gut microbiota, with separate fermentations of EGCG and PCB2 for comparison. The stability of these three compounds under experimental conditions was assessed first. Without the addition of the fecal material, TSA, EGCG, and PCB2 were incubated in the SIEM medium in an anaerobic chamber at 37 °C for 48 h. Approximately 90% of all three compounds (93, 88, and 89%) remained intact after 48 h, suggesting that they were relatively stable in the medium under the experimental conditions. Then, TSA, EGCG, and PCB2, with final concentrations of 50, 100, and 50 μmol/L, respectively, were added into the HFS for anaerobic fermentation. With these concentrations, equal molar amounts of monomeric flavan-3-ol subunits were used as the starting point for fermentation, to facilitate the quantitative comparison of their degradation and the formation of metabolites. The dynamic changes in concentration of the three starting compounds are shown in Figure S4, Supporting Information. EGCG and PCB2 showed fast degradation within a similar time scale. After 2 h, approximately 30% of EGCG and PCB2 were degraded. After 6 h, approximately 89% of EGCG was degraded and it was undetectable after 12 h, whereas PCB2 was almost completely depleted after 6 h. For TSA, a relatively slower degradation was observed. After 6 h, approximately 53% of TSA was degraded and it gradually decreased until the end of fermentation (at 48 h), at which point it was undetectable. Similar rapid initial degradation of EC, catechin, and procyanidins was also observed in other studies.[20,21] These results revealed that all the three flavan-3-ols were degradable by human gut microbiota, but the overall degradation rate of TSA was slower than those of EGCG and PCB2.

Identification and Quantification of Microbial Metabolites of TSA, EGCG, and PCB2. Following the degradation of TSA, EGCG, and PCB2, a series of phenolic metabolites were detected by UHPLC-Q-Orbitrap-MS. A total of 26 metabolites of these three phenolic compounds were tentatively identified. Their corresponding retention times, tentative identification, molecular formulas, detected mass-to-charge ratios (m/z) in negative ionization mode, mass errors ($\Delta m/z$), and concentrations at different fermentation times are shown in Table 1. Comparison of their MS^2 fragments (Table S2, Supporting Information) to previously published data was used for their tentative identification. The concentrations of each metabolite at various time points throughout the fermentation were calculated based on calibration curves of corresponding authentic standards if they were available. The metabolites, for which authentic standards were not available, were quantified using the calibration curves of standards with similar structures. Specifically, TSA was used for the quantification of M01; TSC was used for the quantification of M02 and M03; EGCG, EGC, and EC were used for the quantification of M06, M07, and M08, respectively; PCB2 was used for the quantification of M09−11; 5-(4′-hydroxyphenyl)-valeric acid was used for the quantification of M12−19; and 3-(3′,4′-dihydroxyphenyl)-propionic acid was used for the quantification of M21. Metabolites were divided into upstream and downstream metabolites based on their structure. Metabolites, which retained the characteristic flavan-3-ol structural elements (i.e. intact A and B rings), were defined as upstream metabolites (M01−11), whereas metabolites formed from further degradation of these characteristic structures were defined as downstream metabolites (M12−26). The upstream and downstream phases of metabolism are discussed separately in the following sections.

Upstream Metabolism of TSA. Three unique metabolites (M01−03) were observed in fermentation samples incubated with TSA. The corresponding ions observed in negative mode full MS were 761.13617, 609.12500, and 609.12506, indicating molecular formulas of $C_{37}H_{30}O_{18}$ ($\Delta m/z$ = −0.31), $C_{30}H_{26}O_{14}$ ($\Delta m/z$ = −0.03), and $C_{30}H_{26}O_{14}$ ($\Delta m/z$ = −0.13), respectively. Extracted ion chromatograms of these metabolites over the course of the fermentation are shown in Figure 2. The

https://dx.doi.org/10.1021/acs.jafc.1c00727
J. Agric. Food Chem. 2021, 69, 2477−2484

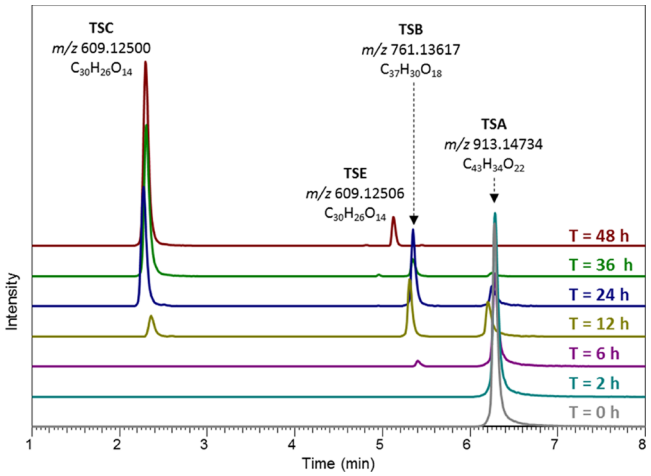

Figure 2. Extracted ion chromatograms of TSA (m/z 913.14734), TSB (m/z 761.13617), TSC (m/z 609.12500), and TSE (m/z 609.12506) in negative ion mode UHPLC-Q-Orbitrap-MS of TSA fermentation samples over 48 h.

mass spectrometric information of these compounds suggested that they might be derived from the degallolylation of TSA through the loss of one or two galloyl groups. In specific, the mass of M01 corresponded to the loss of one galloyl group, which was in accordance with TSB. The masses of M02 and M03 corresponded to the loss of two galloyl groups, which was in accordance with the two stereoisomers theasinensin C and E (TSC and TSE). M02 and M03 had identical HCD fragments (Table S2, Supporting Information), further hinting at the fact that these were indeed a set of stereoisomers. Isomerization of monomeric flavan-3-ols during gut microbiota fermentation was previously reported,[22] thus, we speculate that isomerization of the TSC to TSE may have occurred through the action of a gut microbial isomerase. The identifications of *R*-isomers TSB and TSC in fermentation samples were confirmed by comparing their retention times and mass spectra to the peaks obtained upon degallolylation of TSA (also *R*) by tannase. Thus, M01 is TSB and M02 is TSC, whereas M03 was identified as TSE (*S*-isomer of TSC). It is also worth mentioning that a minor retention time shift (0.07−0.08 min) was observed in the 12 h sample (Figure 2); however, this did not affect identification and subsequent quantification of TSA, TSB, and TSC.

In addition, the degalloylation of TSA resulted in production of gallic acid (M24) and pyrogallol (M26, decarboxylation product of gallic acid) during the fermentation. Ester bond cleavage during microbial fermentation is commonly observed and has been described for various phenolic compounds, such as EGCG, theaflavin digallate, quercetin glycosides, and chlorogenic acids.[23−26] More strikingly, after 48 h of TSA fermentation, high concentrations of TSC and TSE accumulated. In total, these degalloylation products accounted for approximately 93% of the initial amount of TSA, and these compounds did not appear to be subject to further degradation (Figure 2). Moreover, the recalcitrance of the theasinensin backbone to microbial degradation was demonstrated by the fact that the total concentration of TSC and TSE remained stable even after 72 h of fermentation (Figure S5, Supporting Information).

Upstream Metabolism of EGCG and PCB2. The degradation of EGCG and PCB2 resulted in the formation of a total of eight upstream metabolites. Similar to TSA, degalloylation products of EGCG were identified in the EGCG fermentation samples. These degalloylation products were EGC (M04), gallic acid (M24), and pyrogallol (M26). As PCB2 does not contain any galloyl moiety, no degalloylation products were detected. Further degradation of EGCG, EGC, and PCB2 led to the formation of five C-ring opened products in samples incubated with EGCG and PCB2 (Table 1). In specific, M06 (EGCG-derived diphenylpropanol) and M07 (EGC-derived diphenylpropanol) were tentatively identified in the samples incubated with EGCG. For PCB2, M09 (double C-ring opened product of PCB2), M10 (single C-ring opened product of PCB2), and M11 (single C-ring opened and dehydroxylated product of PCB2) were tentatively identified. Note that for M10 and M11, it is unknown which specific positional isomer, with regards to C-ring opening and dehydroxylation, was formed. The extracted ion chromatograms of the C-ring opened products of EGCG and PCB2 at various fermentation times are shown in Figures S6 and S7, supporting information. The *O*1−*C*2 bond in the C-ring of flavan-3-ols is known to be prone to reductive cleavage by several bacteria, such as *Adlercreutzia equolifaciens*, *Asaccharobacter celatus*, and *Slackia equolifaciens*, resulting in the formation of a diphenylpropanols.[27,28] In contrast, C-ring opened products of theasinensins were not detected in samples incubated with TSA, indicating that the C-rings in theasinensins are less prone to reductive cleavage than those in EGCG and PCB2.

EC (M05) and its corresponding C-ring opened derivative (M08) appeared in the PCB2 samples after 2 h of incubation (Figure S8, Supporting Information). The detection of EC, which is the building block of PCB2, indicated that the interflavanic bond of PCB2 was cleaved during the fermentation. These results were in agreement with a previous study in which it was reported that the microbial degradation of PCB2 might proceed through three routes: C-ring opening of the upper unit, interflavanic bond cleavage, and C-ring cleavage plus A-ring fission of the lower unit.[13] However, it was reported that only 10% of PCB2 was converted to EC by the cleavage of the interflavanic bond.[29] This was generally in line with the concentrations of M05 and M08 formed in our fermentations (Table 1). Interestingly, no monomeric flavan-3-ols, such as EGCG, EGC, EC, or their corresponding C-ring opened derivatives, were formed from TSA over the entire course of our fermentation. These results revealed that the interflavanic bond of theasinensins was more recalcitrant to gut microbial degradation than that of PCB2.

Downstream Metabolism of TSA, EGCG, and PCB2. As expected, following the C-ring opening, A-ring fission of monomeric flavan-3-ols was observed. This resulted in the formation of a series of phenyl-γ-valerolactones, phenylvaleric acids, phenyl propionic acids, and their hydroxylated derivatives (Table 1). These results are in agreement with previous reports on these degradation processes.[10,30] Only trace amounts of downstream metabolites of TSA were found, for example, a total of 0.79 μmol/L hydroxyphenylvaleric acids was detected at 48 h. As indicated before, 93% of TSA was converted to TSC (and TSE) via degalloylation by gut microbiota, and no C-ring opening products or monomeric flavan-3-ols were observed. Thus, substantial amounts of the core biphenyl-2,2′,3,3′,4,4′-hexaol moiety remained intact during the 48 h incubation. It is therefore concluded that the downstream metabolism of TSA was negligible, which was in contrast to extensive downstream metabolism of EGCG and

https://dx.doi.org/10.1021/acs.jafc.1c00727
J. Agric. Food Chem. 2021, 69, 2477−2484

PCB2. To gain further insight in the structural and molecular properties underlying these differences, a computational analysis of TSA, TSC, and PCB2 was performed.

Quantum Chemical Calculations of TSA, TSC, and PCB2. In PCB2, the upstream metabolism of cleavage in C-ring O1−C2 bond and interflavanic C−C bond led to further downstream metabolism to form (hydroxylated) phenylcarboxylic acids via subsequent A-ring fission, aliphatic chain shortening, and dehydroxylation. On the other hand, no such C-ring opened or interflavanic C−C bond cleaved metabolites were detected in the fermentation of TSA. Thus, we conclude that the C-ring O1−C2 bond and interflavanic C−C bond in TSA are more recalcitrant than those bonds in PCB2. To gain more insight in these differences in recalcitrance to microbial metabolism, a computational chemistry study was used to obtain more in-depth information on the differences in the chemical structures of PCB2 and TSA. To exclude the potential influence of the galloyl groups of TSA, its non-galloylated equivalent, TSC, has also been computed for comparison. The structures of TSA, TSC, and PCB2 were first optimized and characterized using a DFT method at B3LYP/6-311G(d,p) level of theory in an aqueous phase. The optimized geometries of the three compounds are shown in Figure 3. The

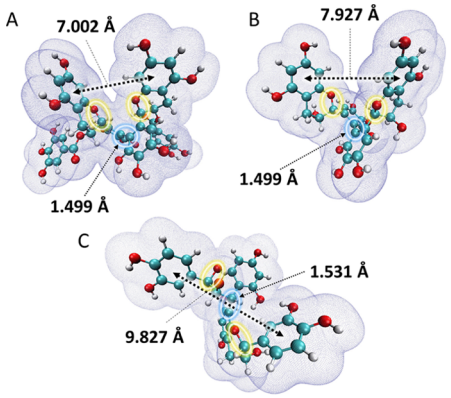

Figure 3. The optimized geometries of TSA (A), TSC (B), and PCB2 (C), and their van der Waals surface (electron density = 0.001 au). The balls in cyan, red, and white represent carbon, oxygen, and hydrogen atoms, respectively. The blue circles represent the interflavanic bonds, where bond lengths are labeled. The yellow circles represent the C-ring O1−C2 bond. The black arrows indicate the distances between the two A rings (TSA and TSC) or B rings (PCB2).

molecular van der Waals surfaces with 0.001 au electron density are also depicted to visualize their difference in stereo-configuration. As demonstrated in Figure 3, apart from the two galloyl groups in TSA, the two theasinensin compounds are present in comparable conformations, especially with regards to the interflavanic C−C bond length of 1.499 Å. The two monomeric catechin subunits in TSA and TSC form a near vertical cross, with dihedral angles (C5′-C6′-C6″-C5″) of −85.89° and −87.81°, respectively. Their C-ring O1−C2 bonds are located in the "interior" of the molecules, facing each other closely. Such spatial arrangement of the catechin subunits may make C-ring O1−C2 bonds less accessible, due to steric hindrance by the other catechin subunit. Unlike theasinensins, the two monomeric catechin subunits in a PCB2 molecule are linked with a dihedral angle (C3-C4-C8′-C7′) of 83.45° and a C−C bond distance of 1.530 Å. This interflavanic C−C bond length is 0.031 Å longer than those of TSA and TSC. Additionally, the shorter interflavanic C−C bond length also makes the theasinensins more compact. The two B rings in PCB2 are pointing in different directions, with a distance of 9.827 Å, whereas the distances of the two A rings in TSA and TSC are 7.002 and 7.927 Å, respectively. Thus, the molecular structure of PCB2 is more extended and open than that of theasinensins. This more extended conformation makes the two C-ring O1−C2 bonds less sterically hindered, especially in the upper unit. Regarding the O1−C2 bond lengths, all three molecules show comparable values (1.440−1.454 Å).

As the bond length of interflavanic C−C bonds of TSA and TSC is noticeably shorter than that of PCB2, it was implicated that the strength of these bonds in TSA and TSC are stronger than that in PCB2. To validate this, bond dissociation enthalpy (BDE) values of these bonds in the three phenolic compounds were computed. The total molecular enthalpies of the three optimized compounds and four optimized corresponding radicals (Figure S9, Supporting Information) were calculated at the same theory level as was used for structure optimization. Using eqs 1−3, it was found that the BDE values of interflavanic C−C bonds in the TSA, TSC, and PCB2 were 452.86, 466.65, and 332.03 kJ/mol, respectively. PCB2 had the lowest BDE value for the interflavanic C−C bond, which was lower by 120.83 kJ/mol (−36.4%) and 134.63 kJ/mol (−40.6%) than those of TSA and TSC, respectively. A lower BDE value is an indication of lower enthalpy change upon homolytic C−C bond cleavage, in other words, it indicates lower bond strength.

Overall, through the quantum chemical calculations of TSA, TSC, and PCB2, it was found that the interflavanic C−C bonds in TSA and TSC were shorter than that of PCB2. Additionally, this C−C bond strength of the theasinensins, as estimated by BDE, was stronger than that of PCB2. Regarding the C-ring O1−C2 bond in each flavan-3-ol subunit, they presented a comparable bond length. Therefore, we argue that the observed different sensitivity to cleavage of this bond between the theasinensins and PCB2 could be explained by their stereo-configuration rather than the O1−C2 bond strength. Based on the optimized configurations calculated by DFT and the overall more compact structure of theasinensins compared to PCB2, we suggest that the C-ring O1−C2 bond in theasinensins is more sterically hindered and may therefore not be accessible to bacterial enzymes. In general, the computational analyses support the experimentally observed differences in the metabolic fates of TSA and PCB2 during gut microbial fermentation.

In conclusion, we investigated the degradation of TSA by human gut microbiota and compared its metabolic fate to EGCG and PCB2. The results indicated that degalloylation occurred readily upon fermentation of TSA, yielding TSC as its main metabolite. In contrast, both EGCG and PCB2 went through more extensive degradation by human gut microbiota to form a series of hydroxylated phenylcarboxylic acids as their main metabolites. The experimentally observed differences in the metabolism of these flavan-3-ols could be explained by the shorter bond length and stronger bond strength of the interflavanic bond in theasinensins, as determined computationally. In addition, the more compact stereo-configuration of theasinensins suggested that steric hindrance may limit degradation of their C-ring by bacterial enzymes during gut microbial fermentation. Our experimental results and the additional structural information obtained from computational

https://dx.doi.org/10.1021/acs.jafc.1c00727
J. Agric. Food Chem. 2021, 69, 2477−2484

analyses shed light on the recalcitrance of theasinensins to degradation by human gut microbiota. It is also noted that a follow-up *in vivo* study is necessary to corroborate the recalcitrance of theasinensins throughout the gastrointestinal tract. Overall, these insights will be of importance for elucidation of the potential health benefits of theasinensins and other black tea phenolics, which possess a biphenyl moiety.

■ ASSOCIATED CONTENT

Supporting Information

The Supporting Information is available free of charge at https://pubs.acs.org/doi/10.1021/acs.jafc.1c00727.

Theasinensin A (TSA) and theaflavin-3,3′-digallate (TFDG) contents in 15 black tea samples and 6 oolong tea samples; mass spectrometric data of metabolites of TSA, EGCG, and PCB2 tentatively identified by UHPLC-Q-Orbitrap-MS; UHPLC-UV280 nm (A1−A3) and UHPLC-MS base peak (B1−B3, negative ionization mode) chromatogram; methods used for flash chromatography and preparative RP-HPLC; high-resolution HCD fragmentation spectrum (NCE=35) of purified TSA innegative and positive ionization mode obtained from UHPLC-Q-Orbitrap-MS; NMR analysis of TSA in acetone-d6; changes in the concentrations of TSA, EGCG, and PCB2 during the fermentation; extracted ion chromatograms of TSC (*m/z* 609.12500) and TSE (*m/z* 609.12506); extracted ion chromatograms of M04 (*m/z* 305.06680), M06 (*m/z* 459.09369), and M07 (*m/z* 307.08252); extracted ion chromatograms of M09 (*m/z* 581.16669), M10 (*m/z* 579.15106), and M11 (*m/z* 563.15613); extracted ion chromatograms of PCB2 (*m/z* 577.13562), M05 (*m/z* 289.07181), and M08 (*m/z* 291.08762); and optimized geometries of the interflavanic bond homolytically fissioned radicals of TSA, TSC, and PCB2 (PDF)

■ AUTHOR INFORMATION

Corresponding Author

Jean-Paul Vincken − *Laboratory of Food Chemistry, Wageningen University, Wageningen 6700 AA, The Netherlands;* orcid.org/0000-0001-8540-4327; Phone: +31-317482234; Email: jean-paul.vincken@wur.nl

Authors

Zhibin Liu − *Laboratory of Food Chemistry, Wageningen University, Wageningen 6700 AA, The Netherlands; Institute of Food Science & Technology, Fuzhou University, Fuzhou 350108, P.R. China*

Wouter J.C. de Bruijn − *Laboratory of Food Chemistry, Wageningen University, Wageningen 6700 AA, The Netherlands;* orcid.org/0000-0003-0564-9848

Mark G. Sanders − *Laboratory of Food Chemistry, Wageningen University, Wageningen 6700 AA, The Netherlands*

Sisi Wang − *Laboratory of Food Chemistry, Wageningen University, Wageningen 6700 AA, The Netherlands*

Marieke E. Bruins − *Food & Biobased Research, Wageningen University & Research, Wageningen 6700 AA, The Netherlands*

Complete contact information is available at: https://pubs.acs.org/10.1021/acs.jafc.1c00727

Notes

The authors declare no competing financial interest.

■ ACKNOWLEDGMENTS

Z.L. acknowledges the financial support from the China Scholarship Council (CSC).

■ ABBREVIATIONS USED

ACN, acetonitrile; BDE, bond dissociation enthalpy; CID, collision-induced dissociation; CPCM, conductor-like polarizable continuum model; DFT, density functional theory; EC, epicatechin; ECG, epicatechin-3-gallate; EGC, epigallocatechin; EGCG, epigallocatechin-3-gallate; ESI, electrospray ionization; FWHM, full width at half maximum; HCD, higher energy C-trap dissociation; HFS, human fecal suspension; HMBC, heteronuclear multiple bond correlation; HSQC, heteronuclear single quantum coherence; PDA, photo diode array; PCB2, procyanidin B2; NMR, nuclear magnetic resonance; SIEM, standard ileal efflux medium; TSA, theasinensin A; TSB, theasinensin B; TSC, theasinensin C; TSE, theasinensin E; UHPLC-Q-Orbitrap-MS, ultrahigh-performance liquid chromatography coupled to hybrid quadrupole Orbitrap mass spectrometry; IT-MS, ion trap mass spectrometry

■ REFERENCES

(1) Vinson, J. A. Black and green tea and heart disease: a review. *BioFactors* **2000**, *13*, 127−132.

(2) Gardner, E. J.; Ruxton, C. H. S.; Leeds, A. R. Black tea−helpful or harmful? A review of the evidence. *Eur. J. Clin. Nutr.* **2007**, *61*, 3−18.

(3) Drynan, J. W.; Clifford, M. N.; Obuchowicz, J.; Kuhnert, N. The chemistry of low molecular weight black tea polyphenols. *Nat. Prod. Rep.* **2010**, *27*, 417−462.

(4) Liu, Z.; Bruins, M. E.; Ni, L.; Vincken, J.-P. Green and black tea phenolics: Bioavailability, transformation by colonic microbiota, and modulation of colonic microbiota. *J. Agric. Food Chem.* **2018**, *66*, 8469−8477.

(5) Hung, W.-L.; Yang, G.; Wang, Y.-C.; Chiou, Y.-S.; Tung, Y.-C.; Yang, M.-J.; Wang, B.-N.; Ho, C.-T.; Wang, Y.; Pan, M.-H. Protective effects of theasinensin A against carbon tetrachloride-induced liver injury in mice. *Food Funct.* **2017**, *8*, 3276−3287.

(6) Hashimoto, F.; Nonaka, G.-I.; Nishioka, I. Tannins and related compounds. LXIX.: Isolation and structure elucidation of B, B'-linked bisflavanoids, theasinensins D-G and oolongtheanin from oolong tea. (2). *Chem. Pharm. Bull.* **1988**, *36*, 1676−1684.

(7) Weerawatanakorn, M.; Hung, W.-L.; Pan, M.-H.; Li, S.; Li, D.; Wan, X.; Ho, C.-T. Chemistry and health beneficial effects of oolong tea and theasinensins. *Food Sci. Hum. Wellness* **2015**, *4*, 133−146.

(8) Miyata, Y.; Tamaru, S.; Tanaka, T.; Tamaya, K.; Matsui, T.; Nagata, Y.; Tanaka, K. Theflavins and theasinensin a derived from fermented tea have antihyperglycemic and hypotriacylglycerolemic effects in KK-A^{y} mice and Sprague−Dawley rats. *J. Agric. Food Chem.* **2013**, *61*, 9366−9372.

(9) Chen, T.; Yang, C. S. Biological fates of tea polyphenols and their interactions with microbiota in the gastrointestinal tract: implications on health effects. *Crit. Rev. Food Sci. Nutr.* **2020**, *60*, 2691−2709.

(10) Mena, P.; Bresciani, L.; Brindani, N.; Ludwig, I. A.; Pereira-Caro, G.; Angelino, D.; Llorach, R.; Calani, L.; Brighenti, F.; Clifford, M. N.; Gill, C. I. R.; Crozier, A.; Curti, C.; Del Rio, D. Phenyl-γ-valerolactones and phenylvaleric acids, the main colonic metabolites of flavan-3-ols: synthesis, analysis, bioavailability, and bioactivity. *Nat. Prod. Rep.* **2019**, *36*, 714−752.

(11) Liu, Z.; de Bruijn, W. J. C.; Bruins, M. E.; Vincken, J.-P. Reciprocal interactions between epigallocatechin-3-gallate (EGCG)

and human gut microbiota in vitro. *J. Agric. Food Chem.* **2020**, *68*, 9804−9815.
(12) Liu, Z.; de Bruijn, W. J. C.; Bruins, M. E.; Vincken, J.-P. Microbial metabolism of theaflavin-3, 3′-digallate and its gut microbiota composition modulatory effects. *J. Agric. Food Chem.* **2021**, *69*, 232−245.
(13) Appeldoorn, M. M.; Vincken, J.-P.; Aura, A.-M.; Hollman, P. C. H.; Gruppen, H. Procyanidin dimers are metabolized by human microbiota with 2-(3, 4-dihydroxyphenyl) acetic acid and 5-(3, 4-dihydroxyphenyl)-γ-valerolactone as the major metabolites. *J. Agric. Food Chem.* **2009**, *57*, 1084−1092.
(14) Tanaka, T.; Watarumi, S.; Matsuo, Y.; Kamei, M.; Kouno, I. Production of theasinensins A and D, epigallocatechin gallate dimers of black tea, by oxidation−reduction dismutation of dehydrotheasinensin A. *Tetrahedron* **2003**, *59*, 7939−7947.
(15) Marteau, C.; Guitard, R.; Penverne, C.; Favier, D.; Nardello-Rataj, V.; Aubry, J.-M. Boosting effect of *ortho*-propenyl substituent on the antioxidant activity of natural phenols. *Food Chem.* **2016**, *196*, 418−427.
(16) Zavitsas, A. A. The relation between bond lengths and dissociation energies of carbon− carbon bonds. *J. Phys. Chem. A* **2003**, *107*, 897−898.
(17) Tao, S.; Chen, G.; Xu, W.; Peng, Y.; Wan, P.; Sun, Y.; Zeng, X.; Liu, Z. Preparation of theasinensin A and theasinensin B and exploration of their inhibitory mechanism on α-glucosidase. *Food Funct.* **2020**, *11*, 3527−3538.
(18) Nonaka, G.; Kawahara, O.; Nishioka, I. A new class of dimeric flavan-3-ol gallates, theasinensins A and B, and proanthocyanidin gallates from green tea leaf. *Chem. Pharm. Bull.* **1983**, *31*, 3906−3914.
(19) Tanaka, T.; Mine, C.; Watarumi, S.; Fujioka, T.; Mihashi, K.; Zhang, Y.-J.; Kouno, I. Accumulation of epigallocatechin quinone dimers during tea fermentation and formation of theasinensins. *J. Nat. Prod.* **2002**, *65*, 1582−1587.
(20) Ou, K.; Sarnoski, P.; Schneider, K. R.; Song, K.; Khoo, C.; Gu, L. Microbial catabolism of procyanidins by human gut microbiota. *Mol. Nutr. Food Res.* **2014**, *58*, 2196−2205.
(21) Chen, W.; Zhu, X.; Lu, Q.; Zhang, L.; Wang, X.; Liu, R. C-ring cleavage metabolites of catechin and epicatechin enhanced antioxidant activities through intestinal microbiota. *Food Res. Int.* **2020**, *135*, 109271.
(22) Hervert-Hernández, D.; Goñi, I. Dietary polyphenols and human gut microbiota: a review. *Food Rev. Int.* **2011**, *27*, 154−169.
(23) Popowski, D.; Pawłowska, K. A.; Piwowarski, J. P.; Granica, S. Gut microbiota-assisted isolation of flavonoids with a galloyl moiety from flowers of meadowsweet, *Filipendula ulmaria* (L.) Maxim. *Phytochem. Lett.* **2019**, *30*, 220−223.
(24) Wang, Y.; Berhow, M. A.; Black, M.; Jeffery, E. H. A comparison of the absorption and metabolism of the major quercetin in brassica, quercetin-3-O-sophoroside, to that of quercetin aglycone, in rats. *Food Chem.* **2020**, *311*, 125880.
(25) Pérez-Burillo, S.; Mehta, T.; Esteban-Muñoz, A.; Pastoriza, S.; Paliy, O.; Rufián-Henares, J. Á. Effect of *in vitro* digestion-fermentation on green and roasted coffee bioactivity: The role of the gut microbiota. *Food Chem.* **2019**, *279*, 252−259.
(26) Chen, H.; Parks, T. A.; Chen, X.; Gillitt, N. D.; Jobin, C.; Sang, S. Structural identification of mouse fecal metabolites of theaflavin 3, 3′-digallate using liquid chromatography tandem mass spectrometry. *J. Chromatogr. A* **2011**, *1218*, 7297−7306.
(27) Takagaki, A.; Nanjo, F. Biotransformation of (−)-epigallocatechin and (−)-gallocatechin by intestinal bacteria involved in isoflavone metabolism. *Biol. Pharm. Bull.* **2015**, *38*, 325−330.
(28) Takagaki, A.; Kato, Y.; Nanjo, F. Isolation and characterization of rat intestinal bacteria involved in biotransformation of (−)-epigallocatechin. *Arch. Microbiol.* **2014**, *196*, 681−695.
(29) Stoupi, S.; Williamson, G.; Drynan, J. W.; Barron, D.; Clifford, M. N. A comparison of the *in vitro* biotransformation of (−)-epicatechin and procyanidin B2 by human faecal microbiota. *Mol. Nutr. Food Res.* **2010**, *54*, 747−759.
(30) Cortés-Martín, A.; Selma, M. V.; Tomás-Barberán, F. A.; González-Sarrías, A.; Espín, J. C. Where to look into the puzzle of polyphenols and health? The postbiotics and gut microbiota associated with human metabotypes. *Mol. Nutr. Food Res.* **2020**, *64*, 1900952.

https://dx.doi.org/10.1021/acs.jafc.1c00727
J. Agric. Food Chem. 2021, 69, 2477−2484